Influence of the Interannual Variability of Vegetation on the Surface Energy Balance—A Global Sensitivity Study

P. GUILLEVIC,*,## R. D. KOSTER,+ M. J. SUAREZ,# L. BOUNOUA,@,& G. J. COLLATZ,& S. O. LOS,** AND S. P. P. MAHANAMA++,+

*Centre d'étude des Environnement Terrestre et Planétaires, Centre National de la Recherche Scientifique, Velizy, France
+Hydrological Sciences Branch, Laboratory for Hydrospheric Science, NASA Goddard Space Flight Center, Greenbelt, Maryland
#Climate and Radiation Branch, Laboratory for Atmospheres, NASA Goddard Space Flight Center, Greenbelt, Maryland
@Department of Meteorology, University of Maryland, College Park, Maryland
&Biospheric Science Branch, NASA Goddard Space Flight Center, Greenbelt, Maryland
**Department of Geography, University of Wales, Swansea, United Kingdom
++Goddard Earth Sciences and Technology Center, UMBC, Baltimore, Maryland

(Manuscript received 11 December 2001, in final form 6 May 2002)

ABSTRACT

The degree to which the interannual variability of vegetation phenology affects hydrological fluxes over land is investigated through a series of simulations with the Mosaic land surface model, run both offline and coupled to the NASA Seasonal-to-Interannual Prediction Project (NSIPP) atmospheric general circulation model (GCM). Over a 9-yr period, from 1982 to 1990, interannual variations of global biophysical land surface parameters (i.e., vegetation density and greenness fraction) are derived from Normalized Difference Vegetation Index (NDVI) data collected by the Advanced Very High Resolution Radiometers (AVHRRs). First the sensitivity of evapotranspiration to interannual variations in vegetation properties is evaluated through offline simulations that ignore feedbacks between the land surface and the atmospheric models, and interannual precipitation variations. Evapotranspiration is shown to be highly sensitive to variations in vegetation over wet continental surfaces that are not densely vegetated. The sensitivity is reduced by a saturation effect over dense vegetation covers and physiological control due to environmental stress over arid and semiarid regions.

Correlations between evapotranspiration and vegetation anomalies are reduced markedly in offline runs that impose interannual variations in both vegetation and precipitation. They are also strongly reduced in the coupled simulations. Although interannual variations in vegetation properties still influence transpiration and interception loss at the global scale in these runs, their impact on large-scale regional climate is much weaker, apparently because the impact is drowned out by atmospheric variability.

1. Introduction

The exchange of moisture and heat between the earth's surface and the atmosphere affects both the dynamics and the thermodynamics of the climate system. In the past two decades, numerical studies [see, e.g., reviews by Mintz (1984), Rowntree (1988), and Garratt (1993)] have shown that the climate system is sensitive to surface hydrological processes through variations in albedo, soil moisture, and surface roughness, all of which are affected by vegetation. Over land, about 50% of heat loss (Chahine 1992) and two-thirds of the water loss (Shukla and Mintz 1982) result from surface evapotranspiration. The hydrological cycle has emerged as one of the key elements in studies of climate change. Prior studies (Sud et al. 1990, 1993; Koster and Suarez 1995; Koster et al. 2000) illustrated that land surface processes contribute significantly to the variance of annual precipitation over continents through water and energy feedbacks with the atmosphere. The potential for precipitation predictability at seasonal timescales has been shown to depend in large part on the ability to forecast the land surface moisture state (e.g., Koster and Suarez 1995; Koster et al. 2000).

However, vegetation phenology (e.g., the seasonal emergence and senescence of leaves, vegetation density, and the green leaf fraction) and land cover also vary interannually in response to climate variability, and these variations may contribute to further climate variability (Charney et al. 1977; Chase et al. 1996; Bonan 1997; Bounoua et al. 2000; Chase et al. 2000). Vegetation extracts moisture from the soil for transpiration, and it has a direct impact on surface albedo and roughness. Vegetation therefore regulates surface fluxes.

Current affiliation: LCPC/Division Eau, Bouguenais, France.

Corresponding author address: Pierre Guillevic, LCPC/Division Eau, Route de Bouaye, B.P. 4129, 44341 Bouguenais Cedex, France. E-mail: pierre.guillevic@lcpc.fr

Changes in vegetation density alter the partition between canopy evapotranspiration (i.e., transpiration plus interception loss), soil evaporation, and runoff.

In this study, we analyze the impact of observed interannual variations in vegetation phenology on surface hydrological processes over a range of spatial scales through a series of numerical experiments made with the Mosaic land surface model (Koster and Suarez 1992), run in both uncoupled mode and coupled to the National Aeronautics and Space Administration (NASA) Seasonal-to-Interannual Prediction Project (NSIPP) atmospheric general circulation model (GCM) (Bacmeister et al. 2000). The interannual variations of vegetation boundary conditions are derived from Normalized Difference Vegetation Index (NDVI) data collected from 1982 to 1990 by the Advanced Very High Resolution Radiometers (AVHRRs) (Sellers et al. 1996a; Los et al. 2000). The NDVI dataset has been used in many climate studies (Randall et al. 1996; Bounoua et al. 2000; Collatz et al. 2000) to evaluate the sensitivity of global climate to changes in vegetation boundary conditions. Through two scenarios, using respectively the maximum and minimum vegetation density over the 9-yr dataset, Bounoua et al. (2000) verify that increasing the vegetation density globally decreases the surface albedo and causes both evapotranspiration and precipitation to increase. Buermann et al. (2001) have shown similar results using the 10-yr monthly pathfinder NDVI dataset.

Many other studies have shown that drastic changes in vegetation induced by land cover change can have a strong influence on local and global simulated climate (Dickinson and Henderson-Sellers 1988; Lean and Warrilow 1989; Shukla et al. 1990; Nobre et al. 1991; Lean and Rowntree 1997; Hoffmann and Jackson 2000; Chase et al. 1996, 2000). However, it is not clear yet whether typical interannual variations in vegetation density have a detectable impact on interannual variations in climate. These presumably more subtle variations are addressed in this paper.

2. Models and data

a. The NSIPP-1 atmospheric GCM

The NSIPP-1 atmospheric GCM (Bacmeister et al. 2000) is the atmospheric component of the NSIPP prediction system. It uses a finite-difference dynamical core based on a C grid in the horizontal and a standard sigma coordinate in the vertical. A detailed description of the core is given in Suarez and Takacs (1995).

The parameterizations of solar and infrared radiative heating rates are those of Chou and Suarez (1999) and (1994), respectively. From the moist physics parameterization, the GCM estimates a cloud fraction at each level. The model uses an empirically based diagnostic cloud scheme in which the cloud cover at each grid point depends directly on the results of the large-scale condensation and convection parameterizations (Bacmeister et al. 2000). For the solar radiation calculation, the GCM levels are then grouped into three regions that are identified, respectively, with high, middle and low clouds. Within each of these regions, clouds are assumed to be maximally overlapped, and the cloud fractions are scaled using a scheme that depends on solar zenith angle and optical thickness.

Turbulence throughout the atmospheric column is modeled using the Louis et al. (1982) scheme. This is a local ''*K*'' scheme with Richardson number–dependent viscosity and diffusivity. Current versions of the model use the gravity-wave drag parameterization of Zhou et al. (1996). Penetrative convection originating in the boundary layer is parameterized using the Relaxed Arakawa–Schubert (RAS) scheme (Moorthi and Suarez 1992).

For the present study, the model was integrated at a resolution of 2.5° longitude × 2° latitude with 34 sigma layers.

b. The Mosaic land surface model

The Mosaic land surface model (Koster and Suarez 1992) computes area-averaged energy and water fluxes from the land surface in response to meteorological forcing. The model allows explicit vegetation control over the computed surface energy and water balances, with environmental stresses acting to increase stomatal resistance and thus reduce the rate of transpiration. The scheme includes a canopy interception reservoir and three soil reservoirs: a thin layer near the surface, a middle layer that encompasses the remainder of the root zone, and a lower ''recharge'' layer for long-term storage. Bare soil evaporation, transpiration, and interception loss occur in parallel, and runoff occurs both as overland flow during precipitation events and as groundwater drainage out of the recharge layer. A complete snow budget is also included. The Mosaic model was originally derived from the Simple Biosphere (SiB) model (Sellers et al. 1986). The model's main innovation is to account for subgrid variability in surface characteristics through the ''mosaic'' approach. A grid square containing several different vegetation types is divided into relatively homogeneous subregions (tiles of the mosaic), each containing a single vegetation and/or bare soil type. The spatial variability of subgrid-scale land surface characteristics has been shown to have a significant impact on surface heat fluxes (Bonan et al. 1993; Li and Avissar 1994).

c. The role of vegetation in the Mosaic model

The surface parameterization includes treatments of albedo, roughness, and surface hydrology (heat transfers and runoff) and is thus influenced by the presence of vegetation and its seasonal and interannual variations. In the model, vegetation regulates transpiration and can-

opy interception loss and thereby controls the partition of surface heat fluxes. At the leaf level, the stomatal conductance that regulates transpiration is assessed using the parameterization of Jarvis (1976). Different environmental stress factors describe the stomata physiology response to the influence of canopy temperature and root zone soil moisture. The integration of the stomatal conductance over the canopy depends on the amount of photosynthetically active radiation (PAR) absorbed by the foliage. Vegetation density regulates light extinction within the canopy and directly affects the integrated stomatal conductance. Therefore, increasing vegetation density enhances transpiration. However, the amount of rainfall intercepted by the canopy also increases with vegetation density and tends to reduce transpiration just after rainstorms.

The surface albedo, which helps determine the net radiation at the surface, is computed with an approximation (Koster and Suarez 1991) to the two-stream radiative transfer model of Sellers (1985) that accounts for canopy structural properties (leaf angle distribution), leaf and soil optical properties, and vegetation density. In the model, the optical properties of vegetation and soils are prescribed from Dorman and Sellers (1989). When the albedo of the soil or the litter under the canopy is higher than that of the leaves, an increase in vegetation density is associated with a decrease in surface albedo and thus with an increase in net radiation.

d. Land surface biophysical parameters

NDVI data from the Global Inventory Monitoring and Modeling System (GIMMS) (Los et al. 1994; Tucker et al. 1994) were used to derive global monthly biophysical land surface datasets from 1982 to 1990 at $1^\circ \times 1^\circ$ resolution (Sellers et al. 1996a; Los et al. 2000). The AVHRR data were adjusted for sensor degradation, volcanic aerosol effects, cloud contamination, solar zenith angle variations, and missing data (Sellers et al. 1996a; Los et al. 2000). We estimated the Leaf Area Index (LAI) and the greenness fraction, the two interannually varying parameters we prescribe in our experiments, using the relations proposed by Sellers et al. (1996a). The LAI is defined as the ratio of leaf area to soil area in a vertical column and thus is a measure of the vegetation density at the surface. The greenness fraction is defined as the fraction of LAI that is photosynthetically active and is thus a measure of the amount of vegetation that regulates canopy transpiration processes. Sellers et al. (1996b) showed evidence of serious cloud contamination in the Tropics (low NDVI values coinciding with persistent cloud cover). The solution to this problem was to raise the NDVI value of ''tropical forest'' pixels to the maximum observed for that pixel during the year. The $1^\circ \times 1^\circ$ dataset is resampled to a ''tile'' resolution using a global vegetation classification map (DeFries and Townshend 1994). The mosaic representation allows us to account for subgrid land cover variability in the 2.5° longitude $\times$ 2° latitude grid defined for the atmospheric GCM.

Our approach to imposing vegetation variability does have limitations. First, variations in vegetation density associated with human-induced changes such as deforestation are included in the satellite record. Our modeling approach, however, does not explicitly account for changes in land use; the cover fraction and vegetation type of each mosaic tile are assumed to be invariant in time. Only the vegetation density (LAI) and the fraction of green leaves within each tile are allowed to vary. Second, the prescribed variability of vegetation density does not alter the seasonal prescription of the surface roughness length, which is independently specified from Dorman and Sellers (1989). Finally, the disaggregation of a $1^\circ \times 1^\circ$ LAI value among the different vegetation tiles in a grid cell could reduce the sensitivity of grid-averaged surface fluxes to LAI variations. If, for example, a grid cell that is half trees and half bare soil has an average LAI (from the NDVI record) of 3, LAIs of 6 and 0 are prescribed for the tree tile and bare soil tile, respectively. Conceivably, evaporation might be more sensitive to LAI values that vary about a mean of 3 for a ''mixed'' biome than to values that vary about 6 and 0 for the separated types, and, in some regions, a mixed biome may be a better description of nature. These limitations should be kept in mind when interpreting the results below.

Averaged values of NDVI-derived LAI for two 3-month periods—December, January and February (DJF), and June, July and August (JJA)—and the associated standard deviations are shown in Fig. 1. During DJF, most of the interannual variation in vegetation density occurs in the Tropics. The maximum standard deviation of LAI for DJF is 1.2 in the Amazon forest, where the LAI varies between 6 and 8. In the northern latitudes, LAI values are small and appear to be significant only over the boreal forests. During JJA, however, the middle and high latitudes exhibit large interannual variations over the boreal forests. The northeastern United States shows the strongest interannual variability in the temperate regions. The interannual variations of seasonal mean LAI are best illustrated in Fig. 2, which shows the seasonally varying LAI anomalies over the 9-yr period for the globe and for two latitudinal bands. Anomalies of total LAI (green and dead leaves) are very similar to those for green LAI (green leaves only). In other words, no significant interannual variations in greenness fraction have been found.

e. Atmospheric data

In the offline experiments, shortwave and longwave incoming radiation, total precipitation, air temperature, air humidity, and wind speed are used to force the land surface model. We extracted these forcings from the atmospheric dataset compiled by the International Satellite Land Surface Climatology Project (ISLSCP) (Sell-

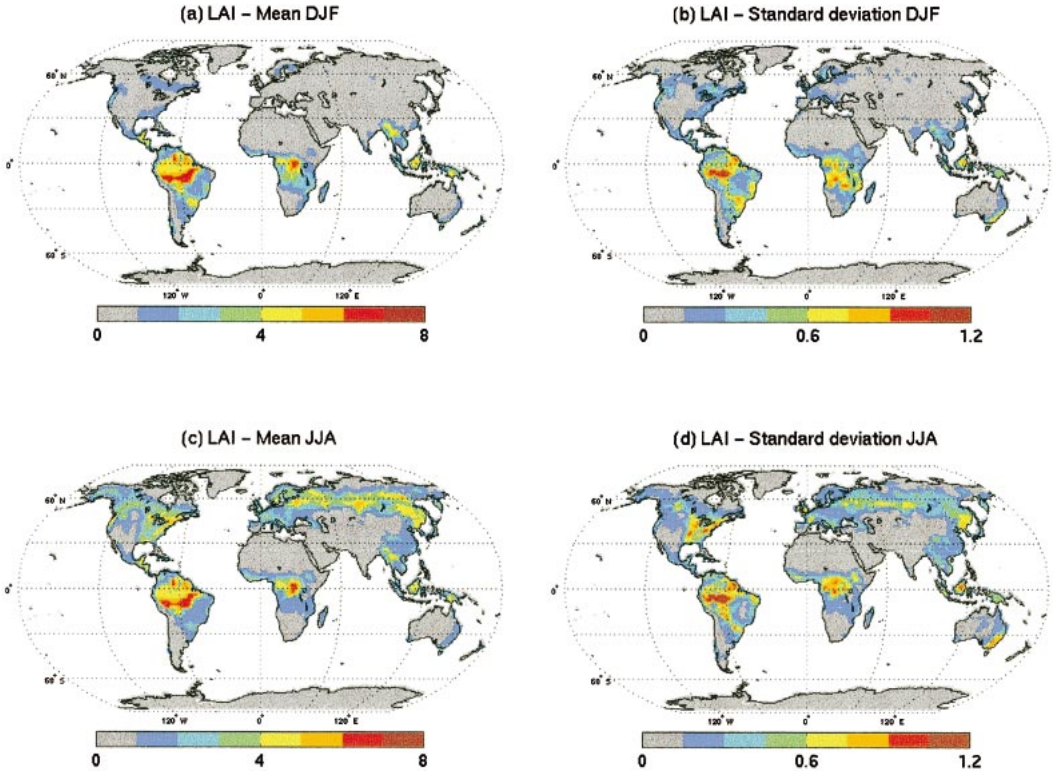

FIG. 1. (a) Mean LAI for Dec–Feb (DJF). (b) Standard deviation of LAI for DJF. (c) Mean LAI for Jun–Aug (JJA). (d) Standard deviation of LAI for JJA.

ers et al. 1996b). This dataset provides meteorological forcing values at 1° resolution every 6 h. These data were resampled at the atmospheric GCM spatial resolution (2.5° longitude × 2° latitude) and then interpolated to a temporal resolution of 20 min. To help isolate the vegetation signal, and since only 2 yr of ISLSCP data are available anyway, the multiyear offline simulations described below use the same 1987 forcing data year after year. Sensitivity of the general nature of our results to the chosen year of forcing is assumed to be small.

As will be seen, some of our simulations do allow the precipitation component of the forcing to vary from year to year. For these simulations, we make use of the 1982–90 monthly precipitation field compiled by the Global Precipitation Climatology Project (GPCP) (Huffman et al. 1995).

3. Experiment design

The objective of this work is to assess the impact of observed interannual variations of vegetation phenology on surface hydrological fluxes, particularly evapotranspiration. Toward this objective, we performed several

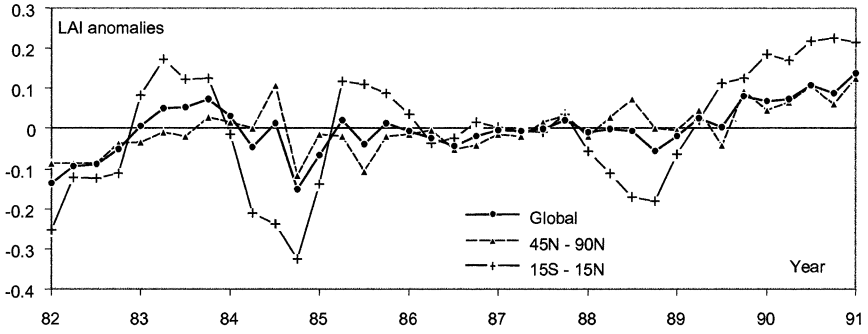

FIG. 2. Seasonal and interannual anomalies of LAI derived from AVHRR measurements. Averages over global land surfaces and over two broad latitudinal bands (45°–90°N and 15°S–15°N) are plotted.

numerical experiments, some using a prescribed atmosphere and others with the coupled land–atmosphere system in order to account for energetic and hydrological feedback processes.

a. Offline experiments

In order to isolate, in a highly controlled setting, the impact of interannual variations of vegetation phenology on surface fluxes, two sets of offline experiments (called OFFLINE1 and OFFLINE2 hereafter) were performed with the Mosaic land surface model.

OFFLINE1 consists of two uncoupled 9-yr simulations. In one simulation (OFFLINE1-Int), the interannual variations of global biophysical land surface parameters derived from the 9-yr NDVI dataset were prescribed. In the other simulation (OFFLINE1-Clim), the associated climatological mean seasonal cycle of these parameters was prescribed. Differences between the two simulations reveal the impact of interannual variations in vegetation phenology. Both OFFLINE1-Int and OFFLINE1-Clim use the same year of prescribed atmospheric forcing (year 1987 from the ISLSCP dataset), repeated nine times.

In the second experiment, OFFLINE2, we performed two similar 9-yr uncoupled simulations, this time using interannual variations in precipitation from 1982 to 1990 derived from monthly GPCP data. For a particular month, precipitation is simply scaled at each time step by a factor $P_{\mathrm{GPCP}}/P_{\mathrm{ISLSCP}}$, where P_{GPCP} and P_{ISLSCP} are the GPCP and ISLSCP precipitation for the month in question, respectively. Note that the spatial and temporal distribution of precipitation in a given month does not change—only the rainfall magnitude is modified. As before, we made one simulation (OFFLINE2-Int) in which the observed interannual variations of vegetation parameters were prescribed and another (OFFLINE2-Clim) in which the associated climatological mean seasonal cycle of these parameters was prescribed. The idea is to see if (a) the effects of vegetation and precipitation variations combine nonlinearly and (b) if the vegetation effects are as noticeable in the presence of another large source of variability.

The energy and water balance calculation requires a description of the initial state of the surface at all spatial grid elements. Since there are no global measurements for the soil moisture initialization, we ran the Mosaic model for a 10-yr period using the 1987 ISLSCP data for the atmospheric forcing and the mean seasonal cycle of vegetation over the period from 1982 to 1990 for the surface boundary conditions. The surface values obtained at the end of the 10-yr ''spinup'' run were used as initial conditions in the two offline experiments.

b. Coupled experiments

In this part of the study, the NSIPP-1 atmospheric GCM was coupled to the Mosaic land surface model. Sea surface temperatures (SSTs) and sea–ice fractions were specified from the monthly Reynolds dataset (Reynolds and Smith 1994); therefore, no ocean model is involved. We ran the NSIPP-1 GCM twice from 1979 to 1990: once with the prescription of interannually varying vegetation parameters (ONLINE-Int) and once with the prescription each year of the climatological mean seasonal cycle of vegetation parameters (ONLINE-Clim). In both simulations, the first 3 yr are disregarded to account for model equilibration. For the 3-yr period for which NDVI data are not available (1979–81), ONLINE-Int used the mean seasonal cycle of vegetation density calculated from 1982 to 1990.

4. Results and discussion

For all experiments, the influence of vegetation variability on surface fluxes was evaluated at different timescales (month, season, year) and for different spatial scales: the GCM grid element scale ($2^\circ \times 2.5^\circ$), the regional scale, over large latitudinal bands, and the global scale. For each area, quantities are averaged over all land points, excluding deserts and ice.

a. Experiment OFFLINE1: 1987 ISLSCP atmospheric forcing

1) GLOBAL SCALE

At the global scale, variations of surface hydrological processes and surface-state variables are well correlated with variations in vegetation boundary conditions. Increasing LAI enhances canopy conductance, transpiration, and total evapotranspiration, and reduces soil evaporation, surface temperature, sensible heat flux, and soil moisture. Global annual differences of yearly surface temperature, total evapotranspiration, and canopy evapotranspiration obtained between OFFLINE1-Int and OFFLINE1-Clim are plotted in Fig. 3. At these time- and space scales (yearly and global average), LAI fluctuations are less than 0.1, and the associated changes in the surface variables are relatively small: interannual variations in total and canopy evapotranspiration are lower than 0.15 and 0.3 W m^{-2}, respectively. Both canopy evapotranspiration and total evapotranspiration differences correlate well with vegetation density anomalies. In the Mosaic model, total evapotranspiration has four components, namely canopy interception loss, transpiration, soil evaporation, and snow sublimation. As LAI increases, the canopy evapotranspiration increases at the expense of the soil component, which makes the canopy evapotranspiration more sensitive to LAI changes than the total evapotranspiration.

2) REGIONAL SCALE

At the regional scale, the influence of vegetation variability is more significant but varies from region to

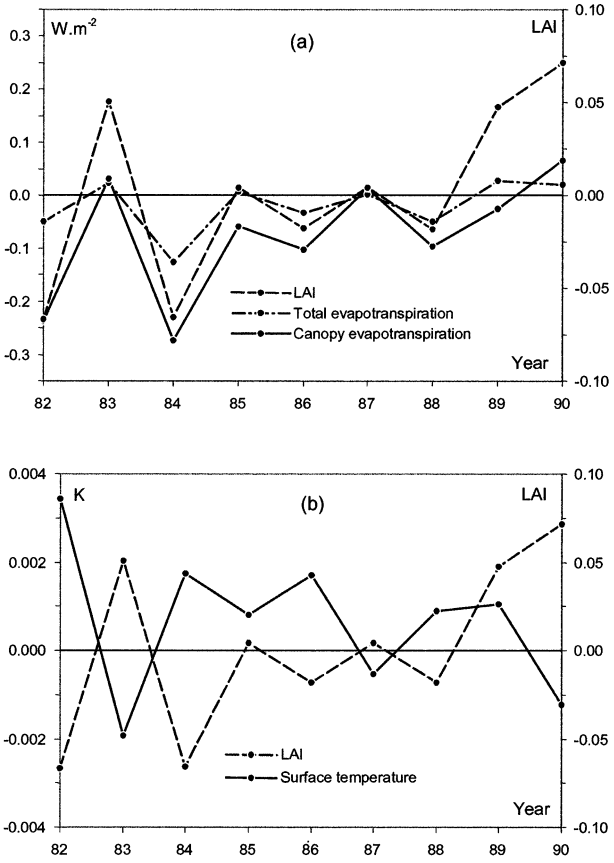

FIG. 3. Experiment OFFLINE1: Global annual differences (OFFLINE1-Int minus OFFLINE1-Clim) in (a) total and canopy evapotranspiration and (b) surface temperature. The dashed lines represent the observed interannual anomalies of LAI.

region. To evaluate the impact of vegetation on local hydrology, we analyzed the variability of water fluxes over nine large-scale regions (see Fig. 4a) representing different ecosystems characterized by different local climates and vegetation densities. The regional areas vary from $6° \times 12°$ (area 1) to $10° \times 50°$ (area 8). Seasonal differences (OFFLINE-Int minus OFFLINE-Clim) in evapotranspiration fluxes obtained between the two simulations are plotted in Fig. 4. Except in two African regions (areas 5 and 6), these differences are highly correlated with LAI anomalies. The impacts of extreme fluctuations of vegetation density (maximum positive and negative anomalies over the 9-yr period) on monthly fluxes in selected regions are reported in Table 1. The highest variations were found over the northeastern United States (area 1) during September 1983. Results for the nine regions suggest that the impact of LAI variations on canopy evapotranspiration is determined by both external environmental factors and internal vegetation factors. We distinguish two main effects: saturation over dense vegetation and water stress.

The influence of LAI variations on latent and sensible heat fluxes was found to be more significant in regions with lower mean LAI. Over the Amazon forest (area 3), an LAI variation of +0.93 (18.9%) had a low impact on latent heat fluxes: +0.72 W m^{-2} (0.6%) for the monthly canopy evapotranspiration and +0.48 W m^{-2} (0.4%) for the total evapotranspiration. Over the eastern United States (area 1), which has a lower mean LAI, a similar variation in LAI (+0.97, or 33.8%) induced higher variations in these fluxes: +3.75 W m^{-2} (6.8%) for the canopy evapotranspiration and +2.8 W m^{-2} (4%) for the total evapotranspiration. The two regions are not subject to high water stress, and their different responses to LAI variations are mainly due to a saturation effect that occurs over dense vegetation covers. In the Mosaic model, the integration over the canopy of the leaf stomatal conductance is based on the computation of the PAR absorbed by the foliage (Sellers 1985). The amount of PAR absorbed by the canopy depends on the vegetation density (LAI) and the vegetation type through various optical and structural properties of the canopy (e.g., cover fraction, tree shape, and leaf angle distribution). The sensitivity of the absorbed PAR to LAI variations is largely reduced for land surfaces characterized by an LAI higher than 4 (Sellers et al. 1996a; Guillevic and Gastellu-Etchegorry 1999). Thus, the sensitivity of the canopy conductance and transpiration to LAI variations is also reduced for LAIs higher than 4.

The second factor that affects the sensitivity of water fluxes to vegetation variations is water stress. Water stress created by low values of soil moisture dramatically decreases transpiration and thus reduces the sensitivity of surface evapotranspiration to LAI variations. Moreover, because the same precipitation is prescribed year after year in experiment OFFLINE1, a relatively high LAI over a dry area in a given year acts (at first) to increase evapotranspiration and thereby to deplete soil moisture relative to other years. Eventually the associated increased water stress acts to restore the increased evapotranspiration to a lower level. Over the two African regions, the annually averaged degree of saturation is less than 0.3, leading to significant water stress. Over West Africa (area 6), for example, an LAI variation of +0.67 (33.1%) had relatively little impact on water fluxes: +0.63 W m^{-2} (0.7%) for the monthly canopy evapotranspiration and only 0.26 W m^{-2} (0.2%) for the total evapotranspiration. Over Europe (area 7), a region that is characterized by a similar LAI but less water stress, a smaller variation in LAI (+0.38, or 18.9%) induced higher variations on water fluxes: +1.44 W m^{-2} (3%) for canopy evapotranspiration and 0.99 W m^{-2} (1.3%) for the total evapotranspiration. The central Africa region (area 5) is subject to a high water stress due to the low precipitation (<5 mm day^{-1}) recorded during 1987. Note that the gauge network over Africa is not dense and may underestimate the rainfall field. Moreover, the year 1987 was subject to an El Niño–Southern Oscillation (ENSO) event. Negative anomalies in precipitation over central Africa are generally observed during El Niño years (Anyamba et al.

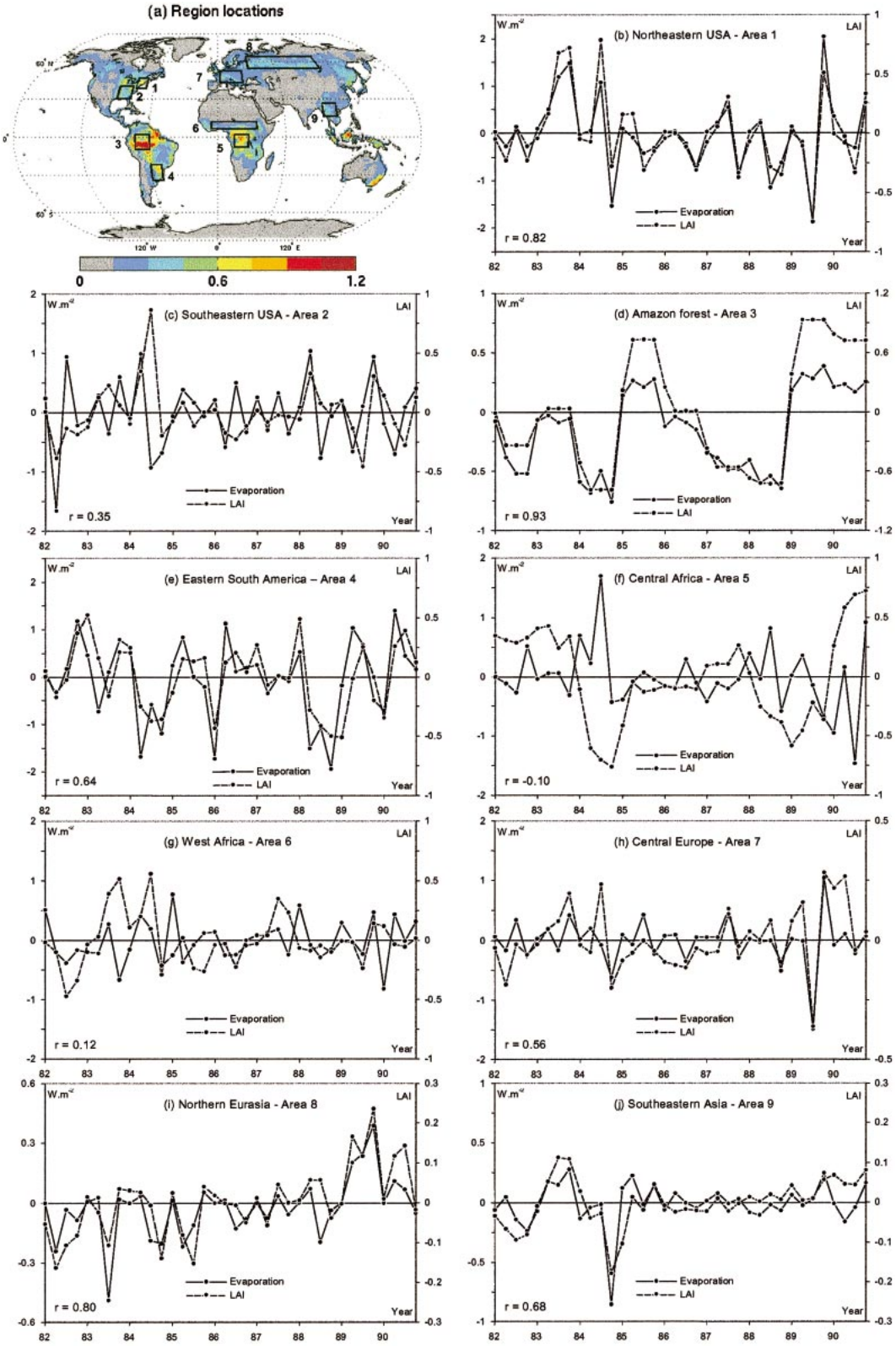

FIG. 4. Experiment OFFLINE1: (a) Locations of the nine selected regions. The map represents the LAI standard deviation over the 9-yr period of observation. (b)–(j) Seasonal evapotranspiration differences (OFFLINE1-Int minus OFFLINE1-Clim). Fluxes are averaged over the nine specific regions. The parameter *r* is the correlation coefficient.

TABLE 1. Impact of extreme fluctuations (maximal positive Δ_{max} and negative Δ_{min} anomalies) on monthly surface fluxes. Absolute and relative variations averaged over five specific regions are presented.

		LAI		Evaporation		Canopy evapotranspiration		Sensible heat	
		$m^2 m^{-2}$	%	W m^{-2}	%	W m^{-2}	%	W m^{-2}	%
Eastern United States (area 1)	Δ_{min}	−0.98	−25.3	−2.47	−2.4	−3.90	−4.5	2.54	7.6
	Δ_{max}	0.97	33.6	2.80	4.0	3.75	6.8	−2.80	−19.1
Amazon (area 3)	Δ_{min}	−0.79	−15.9	−0.81	−0.7	−1.26	−1.3	0.75	6.5
	Δ_{max}	0.93	18.9	0.48	0.4	0.72	0.6	−0.41	−2.5
West Africa (area 6)	Δ_{min}	−0.57	−24.6	−0.76	−0.7	−2.00	−2.1	0.94	2.5
	Δ_{max}	0.67	33.1	0.26	0.2	0.63	0.7	−0.31	−0.7
Europe (area 7)	Δ_{min}	−0.48	−24.7	−2.68	−3.0	−4.57	−7.4	1.84	4.7
	Δ_{max}	0.38	18.9	0.99	1.3	1.44	3.0	−0.88	−2.2
Eastern Europe (area 8)	Δ_{min}	−0.34	−12.1	−0.90	−1.1	−1.57	−2.9	0.88	2.8
	Δ_{max}	0.32	18.6	0.77	2.1	0.83	3.7	−0.48	−5.2

2001). Water stress partly explains why LAI and evapotranspiration anomalies are not well correlated over central and West Africa (see Fig. 4), particularly when looking at seasonal rather than annual totals. Variations in greenness also have some impact on the LAI/evapotranspiration correlations there.

b. Experiment OFFLINE2: 1982–90 monthly GPCP precipitation

One limitation of the OFFLINE1 experiment is that the interannual variations in vegetation density and precipitation were uncoupled. In the real world, periods of higher (lower) precipitation are often associated with periods of higher (lower) vegetation density in regions where soil moisture limits growth. This phenomenon might be expected to reinforce increased evapotranspiration during wet periods and decreased evapotranspiration during dry periods. In other words, correlations between precipitation and vegetation may compound the sensitivity of evapotranspiration to soil moisture.

This limitation is addressed in experiment OFFLINE2. Again, in this experiment, observed interannual variations of precipitation are prescribed. To determine the importance of precipitation/vegetation correlation, we examine the relationship generated in the experiment between soil moisture and evaporation fraction (i.e., the dimensionless ratio of latent heat to net radiation). For a given grid cell in OFFLINE2, we plot the evaporation fraction versus the relative saturation state of soil moisture (the ''degree of saturation'') for each July of the 9 yr. Examples for grid cells in Europe and West Africa are shown in Figs. 5a and 5b. The points for OFFLINE2-Clim are plotted as dark circles, with a solid line fitted through them; the points for OFFLINE2-Int are crosses, and the corresponding fitted line is dashed.

If the compounding effect referred to above is real, then the joint application of observed interannual precipitation and observed LAI variations in OFFLINE2-Int should produce a stronger sensitivity of evaporation ratio to soil moisture than that found in OFFLINE2-Clim; the slope of the fitted line for OFFLINE2-Int should be larger, since wetter conditions would tend to coincide with higher LAI. We observe such a tendency over Europe (see Fig. 5a). Nevertheless, this effect is generally weak over most parts of the globe. As seen in Fig. 5b, for example, little evidence of a compounding effect is seen in West Africa. Across almost the whole globe, applying observed fields of precipitation and LAI does not result in significantly increased evapotranspiration sensitivity to soil moisture. This is, in fact, consistent with a generally low correlation seen in the data between GPCP precipitation variations and NDVI-derived fluctuations in vegetation properties.

Seasonal variations of LAI and evapotranspiration anomalies obtained in OFFLINE2 over eastern North America (area 1) and the Amazon forest (area 3) are presented in Figs. 5c and 5d, respectively. Comparing these results to those from experiment OFFLINE1 (see Fig. 4), we see that accounting for interannual variations in precipitation significantly decreases correlations between LAI and evapotranspiration anomalies. These results, which are typical, suggest that simulated water fluxes are more sensitive to precipitation variations than to vegetation density variations. Precipitation variations that are uncorrelated with vegetation state ''swamp out'' the vegetation signal.

To summarize both offline experiments, the experimental design allows us to isolate and quantify the impact of realistic vegetation density variability on evapotranspiration. Results from OFFLINE1 show that under particular circumstances (low to moderate mean LAI and low water stress) vegetation fluctuations could have a significant impact on evapotranspiration. However, experiment OFFLINE2 shows that this effect is generally much less than that associated with rainfall variability. Of course, in the real world, vegetation development and climate are highly coupled through the exchange of moisture, heat, and momentum at the land–atmosphere interface (Sud et al. 1993). This coupling can lead to important correlations between vegetation state and various atmospheric forcing variables (e.g., precipitation, air temperature, specific humidity, and incident radiation). We treat none of these correlations in OFFLINE1

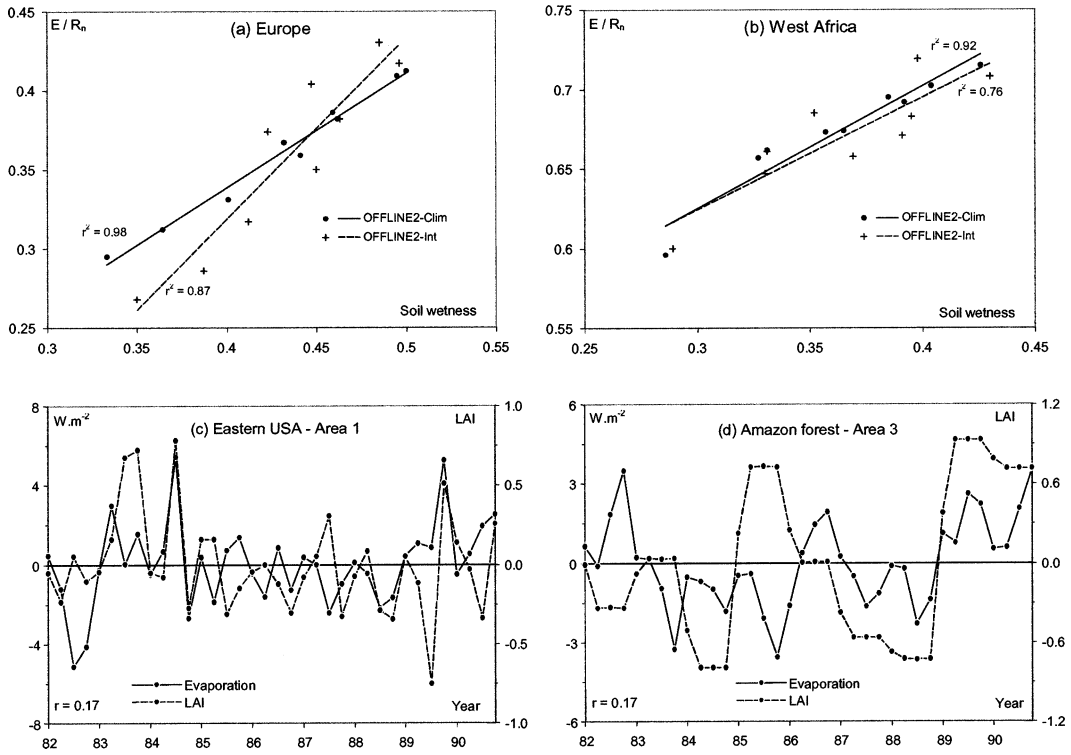

FIG. 5. Experiment OFFLINE2: (a) Evaporation fraction (dimensionless ratio of latent heat to net radiation) vs degree of saturation in the root zone (dimensionless) obtained for each Aug of the 9-yr period for a grid cell over Europe. (b) Same as (a), but for West Africa. (c) Seasonal differences (OFFLINE2-Int minus OFFLINE2-Clim) of evapotranspiration (solid line) and LAI (dotted line) for the northeastern United States. (d) Same as (c), but for the Amazonian forest. The parameter r is the correlation coefficient.

and only the precipitation/vegetation correlation in OFFLINE2, in effect making the assumption that this is the most important correlation. Because this assumption may be invalid, we present, in the next section, the analysis in which the NSIPP-1 atmospheric GCM coupled to the Mosaic land surface model is used to simulate the atmosphere's behavior and response to surface anomalies. Although the coupled experiment does not treat the simultaneous evolution of vegetation and climate properties, it does allow us to take into account the effects of vegetation state on atmospheric forcing variables.

c. Experiment ONLINE: Coupled land–atmosphere simulations

Although the statistical analysis of experiment ONLINE is limited by the use of only 9 yr of vegetation data, the short dataset should nevertheless be adequate to illustrate strong impacts of vegetation on climate, if they exist. Los et al. (2001) detected two statistically significant modes of interannual NDVI variations during the 9-yr period of satellite observations used in this study. One mode has a period of 2.6 yr that closely corresponds to variations in the ENSO index during the 1980s, and the other mode has a period of 3.4 yr that corresponds well with the period of the North Atlantic Oscillation (NAO) index during the 1980s.

The interannual variability of evapotranspiration and precipitation in simulations ONLINE-Clim and ONLINE-Int is illustrated in Figs. 6a–c. The evapotranspiration variances obtained in the two simulations are very similar in magnitude and spatial structure (see Figs. 6a,b), suggesting that they are not affected much by vegetation variability. Globally, the correlations between the prescribed interannual anomalies in LAI and the simulated interannual anomalies in GCM climate variables are weak. In Figs. 6e and 6f, we show the correlation coefficients obtained between the LAI and both canopy evapotranspiration and convective precipitation. Large-scale precipitation anomalies are very weak and are not represented in the figure. Correlations between LAI and canopy evapotranspiration are generally lower than 0.5. Correlations between the anomalies of LAI and convective precipitation are generally insignificant. In contrast, correlations between precipitation and evapotranspiration anomalies are much higher across the globe (see Fig. 6d). The time series of LAI and evapotranspiration anomalies obtained over eastern North America (area 1) and the Amazon forest (area 3) are represented in Figs. 6g and 6h, respectively. A comparison of these time series with those from experiment

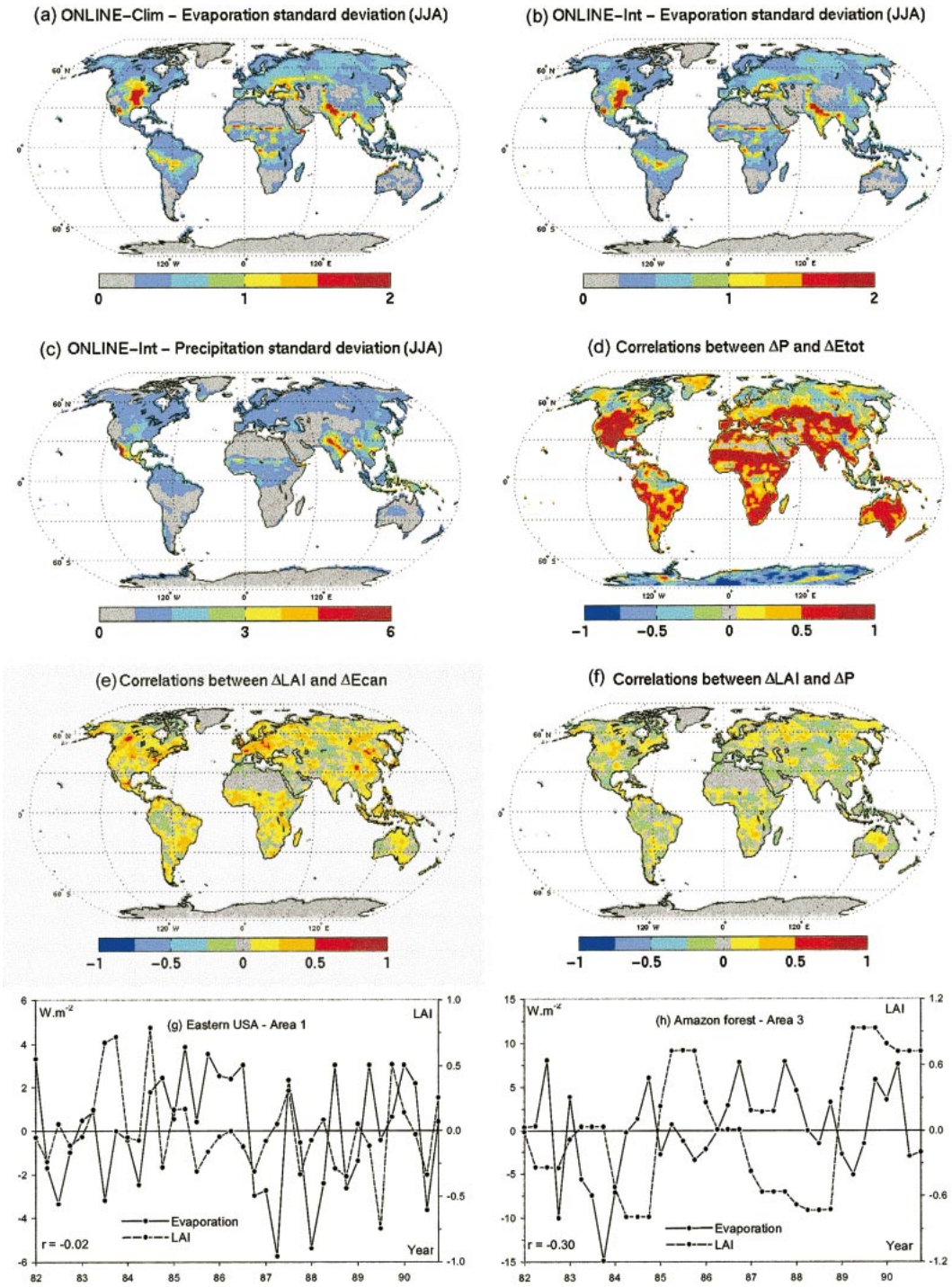

FIG. 6. Experiment ONLINE: (a) Standard deviation of evapotranspiration (mm day^{-1}) obtained in ONLINE-Clim for JJA of the 9-yr period. (b) Same as (a), but obtained in ONLINE-Int. (c) Same as (b), but for precipitation (mm day^{-1}). (d) Correlation coefficients between precipitation and total evapotranspiration anomalies obtained in ONLINE-Int. (e) Correlation coefficients between LAI anomalies and anomalies in canopy evapotranspiration (ΔE_{can}) obtained in ONLINE-Int. (f) Same as (e), but for convective precipitation (ΔP). (g) Seasonal variation of evapotranspiration (solid lines) and LAI (dotted lines) anomalies obtained over the northeastern United States. (h) Same as (g), but for the Amazonian forest. The parameter r is the correlation coefficient.

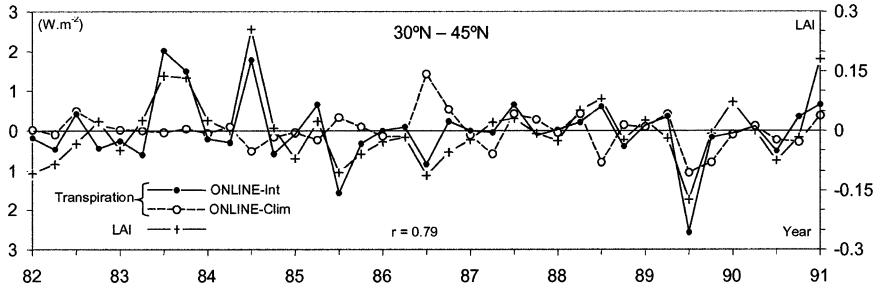

FIG. 7. Experiment ONLINE: Seasonal anomalies of LAI and transpiration obtained with both simulations ONLINE-Int and ONLINE-Clim over the latitudinal band 30°–45°N. The parameter *r* is the correlation coefficient between LAI and ONLINE-Int transpiration.

OFFLINE1 (see Fig. 4) shows that including a dynamic atmosphere seriously decreases LAI/surface flux correlations. We found similar results in OFFLINE2, the experiment that accounts for observed interannual precipitation fluctuations.

At the global scale or for different latitude bands, the correlations between LAI and evapotranspiration are also generally weak. The highest correlations with LAI are obtained for transpiration, but the values depend strongly on the region considered. Over the band 30°–45°N, the correlation coefficient calculated between LAI and transpiration anomalies in ONLINE-Int is 0.79 (see Fig. 7). Conversely, except for two time periods (JJA in 1986 and 1989), the variation of spatially averaged transpiration in ONLINE-Clim is weak. Thus, for this part of the globe, we do see evidence of an impact of LAI variability.

Year-to-year anomalies of LAI, convective precipitation, canopy evapotranspiration, and total evapotranspiration from experiment ONLINE-Int, averaged over all land surfaces, are presented in Fig. 8. Recall that in OFFLINE1-Int, yearly global canopy and total evapotranspiration are clearly correlated to vegetation density (see Fig. 3). In ONLINE-Int, the yearly global canopy evapotranspiration is also highly correlated to LAI (see Fig. 8); the amplitude of the LAI impact is very similar in the two experiments. However, the total evapotranspiration, which is what the GCM's atmosphere sees, is much more connected to interannual variations of rainfall than to interannual variations in LAI.

We are forced to conclude that variations in hydrological fluxes (in particular, variations in precipitation and total evapotranspiration) mostly reflect interannual variability in the atmospheric GCM's ''weather'' and that variations caused by LAI variability are much smaller. In other words, the influence of vegetation phenology variations on climate can be drowned out by the atmosphere's own variability.

A possible limitation to simulation ONLINE-Int is the lack of any correlation from year to year between precipitation at a grid cell and the vegetation density in that cell. In ONLINE-Int, interannual variations in vegetation boundary conditions are derived from radiometric observations, whereas interannual variations in precipitation, though controlled in part by the prescribed SSTs, are largely a function of random atmospheric processes. A grid cell may easily experience lower-than-average precipitation and thus lower-than-average soil moisture during a year of higher-than-average LAI. Note that this does not imply a deficiency in the coupled model. Because of atmospheric chaos, even a ''perfect'' coupled model could not be expected to reproduce ob-

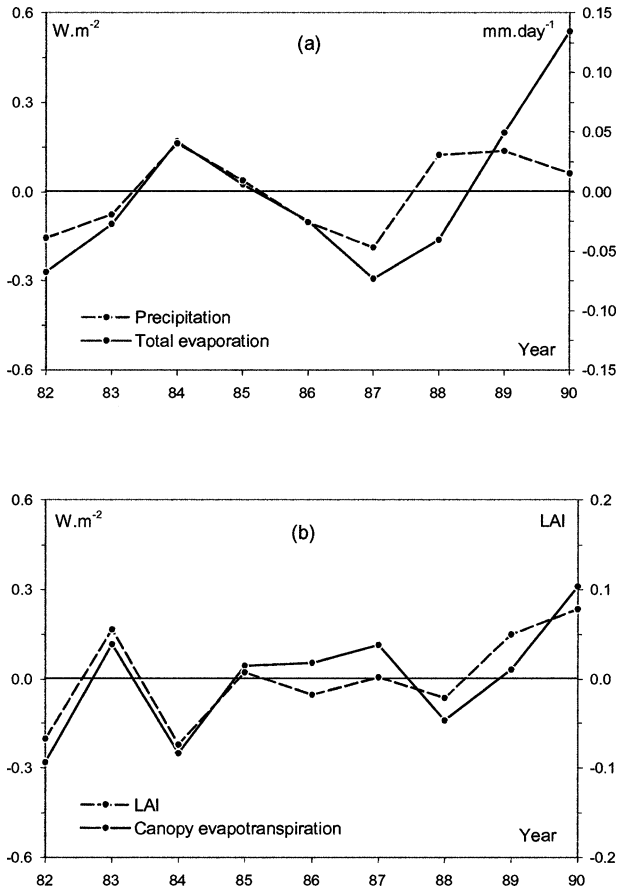

FIG. 8. Simulation ONLINE-Int: Yearly averaged anomalies of (a) precipitation and total evapotranspiration, and (b) LAI and canopy evapotranspiration. All quantities are averaged over the globe.

served precipitation anomalies in a specified year of simulation, particularly over midlatitude continents.

Experiment OFFLINE2 suggested that the impact of the precipitation/vegetation correlation is small. Nevertheless, the observational datasets underlying that experiment may be imperfect; they may underestimate the strength of the correlation and thus its impact on evapotranspiration. Furthermore, the link between vegetation and all climate variables (e.g., between vegetation and radiation or vegetation and temperature) in experiment ONLINE is treated in only one direction: vegetation can affect the simulated climate variables, but these variables cannot in turn influence the growth or senescence of the vegetation. As a result, the coupled experiment above may underestimate the impact of vegetation variations on climate. A dynamic vegetation model, one that allows LAI and seasonal weather to evolve together, might induce a stronger signal.

5. Summary

The Mosaic land surface model, run both in offline mode and coupled to the NSIPP-1 atmospheric GCM, is used to investigate the sensitivity of global and regional climate to observed interannual variability in vegetation boundary conditions (i.e., LAI and greenness fraction). Vegetation phenology was derived from satellite observations for 1982–90.

To isolate the sensitivity of the Mosaic land surface model to vegetation density variations, we constructed an idealized offline experiment (OFFLINE1) in which the vegetation properties—but not the atmospheric forcing—varied from year to year. The influence of vegetation variability on water fluxes is significant but depends largely on the region considered. Results obtained over nine large-scale regions show that the impact of vegetation density variability tends to be reduced by a saturation effect over dense vegetation cover and by stomatal physiology in regions of high soil water stress.

A second offline experiment (OFFLINE2), in which precipitation as well as vegetation properties vary interannually, shows that precipitation variability has an even stronger impact on surface fluxes than does variability in vegetation phenology. This result is echoed in an experiment performed with the land surface model coupled to the atmospheric GCM. In the coupled experiment, when the anomalies of vegetation phenology and canopy evapotranspiration (i.e., transpiration plus interception loss) are averaged over the globe or across large-scale regions, we do see a significant correlation between them. The degree of correlation, however, is significantly reduced at regional scales, for which phenology effects are drowned out by atmospheric variability. At regional scales, interannual variations of surface evapotranspiration are much more correlated to rainfall fluctuations.

Our results are somewhat limited by various aspects of the experimental design. The statistical analysis, for example, is limited by the fact that only 9 yr of data are examined. The presented sensitivities are for a specific land surface model and may differ from those obtained with other models. In addition, the various fields that control evapotranspiration in the real world (e.g., precipitation, vegetation, air temperature, humidity, radiation, and wind speed) interact with each other freely and may be characterized by significant correlation, correlation that could amplify the effects of the vegetation variability. We address the precipitation/vegetation correlation effect in experiment OFFLINE2, making the implicit assumption that this should be the largest correlation effect, but find that its importance appears minor. Nevertheless, the test is not conclusive, and the other, untested correlations may be relevant. The incorporation of a dynamic vegetation model that allows vegetation to vary consistently with the seasonal climate is thus an appropriate avenue for further research.

Acknowledgments. This research, which was funded by the Earth Science Enterprise of NASA Headquarters through the NASA Seasonal-to-Interannual Prediction Project (NSIPP), was performed while the lead author worked at NASA Goddard Space Flight Center (NASA GSFC) as an employee of the Goddard Earth Sciences and Technology Center (GEST UMBC).

REFERENCES

Anyamba, A., C. J. Tucker, and J. R. Eastman, 2001: NDVI anomaly patterns over Africa during the 1997/98 warm ENSO event. *Int. J. Remote Sens.*, **22,** 1847–1859.

Bacmeister J., P. J. Pegion, D. S. Siegfried, and M. J. Suarez, 2000: Atlas of seasonal means simulated by the NSIPP 1 atmospheric GCM. NASA Tech. Memo. 2000-104606, M. J. Suarez, Ed., Vol. 17, Technical Report Series on Global Modeling and Data Assimilation, 194 pp. [Available from NASA Center for Aerospace Information, 800 Elkridge Landing Rd., Linthicum Heights, MD 21090-2934.]

Bonan, G. D., 1997: Effects of land use on the climate of the United States. *Climatic Change,* **37,** 449–486.

——, D. Pollard, and S. L. Thompson, 1993: Influence of sub-grid scale heterogeneity in leaf area index, stomatal resistance, and soil moisture on grid-scale land–atmosphere interactions. *J. Climate,* **6,** 1882–1897.

Bounoua, L., G. J. Collatz, S. O. Los, P. J. Sellers, D. A. Dazlich, C. J. Tucker, and D. A. Randall, 2000: Sensitivity of climate to changes in NDVI. *J. Climate,* **13,** 2277–2292.

Buermann, W., J. Dong, X. Zeng, R. B. Myneni, and R. E. Dickinson, 2001: Evaluation of the utility of satellite-based vegetation leaf area index data for climate simulations. *J. Climate,* **14,** 3536–3550.

Chahine, M. T., 1992: The hydrology cycle and its influence on climate. *Nature,* **359,** 373–380.

Charney, J. G., W. J. Quirk, S. H. Chow, and J. Kornfield, 1977: A comparative study of the effects of albedo change in drought in semi-arid regions. *J. Atmos. Sci.,* **34,** 1366–1385.

Chase, T. N., R. A. Pielke, T. G. F. Kittel, R. Nemani, and S. W. Running, 1996: Sensitivity of a general model to global changes in leaf area index. *J. Geophys. Res.,* **101,** 7393–7408.

——, ——, ——, ——, and ——, 2000: Simulated impacts of historical land cover changes on global climate in northern winter. *Climate Dyn.,* **16,** 93–105.

Chou, M. D., and M. J. Suarez, 1994: An efficient thermal infrared

radiation parameterization for use in general circulations models. NASA Tech. Memo. 104606, Vol. 10, 84 pp. [Available from NASA Center for Aerospace Information, 800 Elkridge Landing Rd., Linthicum Heights, MD 21090-2934.]

——, and ——, 1999: A solar radiation parameterization for atmospheric studies. NASA Tech. Memo. 104606, Vol. 11, 40 pp. [Available from NASA Center for Aerospace Information, 800 Elkridge Landing Rd., Linthicum Heights, MD 21090-2934.]

Collatz, G. J., L. Bounoua, S. O. Los, D. A. Randall, I. Y. Fung, and P. J. Sellers, 2000: A mechanism for the influence of vegetation on the response of the diurnal temperature range to changing climate. *Geophys. Res. Lett.,* **27,** 3381–3384.

DeFries, R. S., and J. R. G. Townshend, 1994: NDVI-derived land cover classification at global scales. *Int. J. Remote Sens.,* **15,** 3567–3586.

Dickinson, R. E., and A. Henderson-Sellers, 1988: Modeling tropical deforestation: A study of GCM land-surface parameterizations. *Quart. Trans. Roy. Meteor. Soc.,* **114,** 439–462.

Dorman, J. L., and P. J. Sellers, 1989: A global climatology of albedo, roughness length and stomatal resistance for atmospheric general circulation models as represented by the Simple Biosphere Model (SiB). *J. Appl. Meteor.,* **28,** 833–855.

Garratt, J. R., 1993: Sensitivity of climate simulations to land-surface and atmospheric boundary-layer treatments—A review. *J. Climate,* **6,** 419–449.

Guillevic, P., and J. P. Gastellu-Etchegorry, 1999: Modeling BRF and radiation regime of tropical and boreal forests. Part II: PAR regime. *Remote Sens. Environ.,* **68,** 317–340.

Hoffmann, W. A., and R. B. Jackson, 2000: Vegetation–climate feedbacks in the conversion of tropical savanna to grassland. *J. Climate,* **13,** 1593–1602.

Huffman, G. J., R. F. Adler, B. Rudolf, U. Schneider, and P. R. Keehn, 1995: Global precipitation estimates based on a technique for combining satellite-based estimates, rain gauge analysis, and NWP model precipitation information. *J. Climate,* **8,** 1284–1295.

Jarvis, P., 1976: The interpretation of the variations in leaf water potential and stomatal conductance found in canopies in the field. *Philos. Trans. Roy. Soc. London,* **273,** 593–610.

Koster, R. D., and M. J. Suarez, 1991: A simplified treatment of SiB's land surface albedo parameterization. NASA Tech. Memo. 104538, Washington, DC, 11 pp.

——, and ——, 1992: Modeling the land surface boundary in climate models as a composite of independent vegetation stands. *J. Geophys. Res.,* **97,** 2697–2715.

——, and ——, 1995: Relative contributions of land and ocean processes to precipitation variability. *J. Geophys. Res.,* **100,** 13 775–13 790.

——, ——, and M. Heiser, 2000: Variance and predictability of precipitation at seasonal-to-interannual timescales. *J. Hydrometeor.,* **1,** 26–46.

Lean J., and D. A. Warrilow, 1989: Simulation of the regional climatic impact of Amazon deforestation. *Nature,* **342,** 411–413.

——, and P. R. Rowntree, 1997: Understanding the sensitivity of a GCM simulation of Amazonian deforestation to the specification of vegetation and soil characteristics. *J. Climate,* **10,** 1216–1235.

Li, B., and R. Avissar, 1994: The impact of spatial variability of land-surface characteristics on land surface heat fluxes. *J. Climate,* **7,** 527–537.

Los, S. O., C. O. Justice, and C. J. Tucker, 1994: A global 1° by 1° NDVI dataset for climate studies derived from the GIMMS continental NDVI. *Int. J. Remote Sens.,* **15,** 3289–3295.

——, and Coauthors, 2000: A global 9-yr biophysical land surface dataset from NOAA AVHRR data. *J. Hydrometeor.,* **1,** 183–199.

——, G. J. Collatz, L. Bounoua, P. J. Sellers, and C. J. Tucker, 2001: Global interannual variations in sea surface temperature and land surface vegetation, air temperature, and precipitation. *J. Climate,* **14,** 1535–1549.

Louis, J., M. Tiedke, and J. Geleyn, 1982: A short history of the PBL parameterization at ECMWF. *Proc. ECMWF Workshop on Planetary Boundary Layer Parameterization,* Reading, United Kingdom, ECMWF, 59–80.

Mintz, Y., 1984: The sensitivity of numerically simulated climates to land-surface boundary conditions. *The Global Climate,* J. Houghton, Ed., Cambridge University Press, 79–105.

Moorthi, S., and M. J. Suarez, 1992: Relaxed Arakawa–Shubert: A parameterization of moist convection for general circulation models. *Mon. Wea. Rev.,* **120,** 978–1002.

Nobre, C. A., P. J. Sellers, and J. Shukla, 1991: Amazonian deforestation and regional climate change. *J. Climate,* **4,** 957–987.

Randall, D. A., and Coauthors, 1996: A revised land surface parameterization (SiB2) for GCMs. Part III: The greening of the Colorado State University general circulation model. *J. Climate,* **9,** 738–763.

Reynolds, W. R., and T. M. Smith, 1994: Improved global sea surface temperatures analyses using optimum interpolation. *J. Climate,* **7,** 929–948.

Rowntree, P. R., 1988: Review of GCMs as a basis for predicting the effects of vegetation change on climate. *Forests, Climate, and Hydrology—Regional Impacts,* E. R. C. Reynolds and F. B. Thompson, Eds., United Nations Publications, 162–196.

Sellers, P. J., 1985: Canopy reflectance, photosynthesis and transpiration. *Int. J. Remote Sens.,* **6,** 1335–1372.

——, Y. Mintz, Y. C. Sud, and A. Dalcher, 1986: A simple biosphere model (SiB) for use within general circulation models. *J. Atmos. Sci.,* **43,** 305–331.

——, S. O. Los, C. J. Tucker, C. O. Justice, A. D. Dazlich, G. J. Collatz, and D. A. Randall, 1996a: A revised parameterization (SiB2) for atmospheric GCMs. Part II: The generation of global fields of terrestrial biophysical parameters from satellite data. *J. Climate,* **9,** 706–737.

——, and Coauthors, 1996b: The ISLSCP Initiative I global data sets: Surface boundary conditions and atmospheric forcings for land–atmosphere studies. *Bull. Amer. Meteor. Soc.,* **77,** 1987–2005.

Shukla, J., and Y. Mintz, 1982: Influence of land surface evapotranspiration on the earth's climate. *Science,* **215,** 1498–1500.

——, C. Nobre, and P. Sellers, 1990: Amazon deforestation and climate change. *Science,* **247,** 1322–1325.

Suarez, M. J., and L. L. Takacs, 1995: Documentation of the ARIES/GEOS Dynamical Core: Version 2. NASA Tech. Memo. 104606, Vol. 5, 45 pp. [Available from NASA Center for Aerospace Information, 800 Elkridge Landing Rd., Linthicum Heights, MD 21090-2934.]

Sud, Y. C., P. J. Sellers, Y. Mintz, M. D. Chou, G. K. Walker, and W. E. Smith, 1990: Influence of the biosphere on the global circulation and hydrologic cycle—A GCM simulation experiment. *Agric. For. Meteor.,* **52,** 133–180.

——, W. C. Chao, and G. K. Walker, 1993: Dependence of rainfall on vegetation: Theoretical considerations, simulation experiments, observations and inferences from simulated atmospheric soundings. *J. Arid Environ.,* **25,** 5–18.

Tucker, C. J., H. E. Dregne, and W. W. Newcomb, 1994: AVHRR datasets for determination of desert spatial extent. *Int. J. Remote Sens.,* **15,** 3547–3565.

Zhou, J., Y. C. Sud, and K. M. Lau, 1996: Impact of orographically induced gravity wave drag in the GLA GCM. *Quart. J. Roy. Meteor. Soc.,* **122,** 903–927.